

Experimental search for nonstrange narrow isovector dibaryons

B. Tatischeff, P. Berthet, M. P. Combes-Comets, J. P. Didelez,
R. Frascaria, and Y. Le Bornec
Institut de Physique Nucléaire, F-91406 Orsay Cedex, France

A. Boudard, J. M. Durand, M. Garcon, J. C. Lugol, and Y. Terrien
*Departement de Physique Nucléaire à Moyenne Energie, Centre d'Etudes Nucléaires de Saclay,
F-91191 Gif-sur-Yvette Cedex, France*

R. Beurtey and L. Farvacque
Laboratoire National Saturne, Centre d'Etudes Nucléaires de Saclay, F-91191 Gif-sur-Yvette Cedex, France
(Received 27 March 1987)

Missing mass spectra from ${}^3\text{He}(p,d)X$ at $T_p=0.75$ GeV ($\theta_{\text{lab}}=22^\circ, 32^\circ, \text{ and } 40^\circ$) and $T_p=0.925$ GeV ($\theta_{\text{lab}}=30^\circ$ and 40°) have been measured. Missing mass spectra from $p({}^3\text{He},d)X$ at $T_{{}^3\text{He}}=2.7$ GeV and $\theta_{\text{lab}}=18^\circ$ have also been measured. The experiments have been carried out with a high missing mass resolution in order to detect possible narrow structures associated with $B=2, T=1$ quantum numbers. Such structures have been seen, with the following masses and widths:

$$M_x = 2.240 \pm 0.005, \quad (\Gamma_{1/2} \approx 0.016 \pm 0.003) \text{ GeV},$$

$$M_x = 2.192 \pm 0.003, \quad (\Gamma_{1/2} \approx 0.025 \pm 0.006) \text{ GeV},$$

and

$$M_x = 2.121 \pm 0.003, \quad (\Gamma_{1/2} \approx 0.025 \pm 0.002) \text{ GeV}.$$

A broad structure with mass close to $M_x \approx 2.17$ GeV, the mass of free $N+\Delta$, and a width close to $\Gamma_{1/2} \approx 0.1$ GeV is observed. The observed peaks might be related to six-quark states.

I. INTRODUCTION

The spectroscopy of dibaryonic resonances has been strongly stimulated over the last ten years, by theoretical as well as experimental studies. It was shown that six quarks confined in a bag, produce as a consequence many exotic states¹ neither predicted before nor experimentally observed. At the same time, nucleon-nucleon experiments from Argonne National Laboratory-Zero Gradient Synchrotron (ANL-ZGS) and deuteron photodisintegration from Tokyo revealed unexpected features which were related to dibaryonic resonances.

The NN studies started at ANL (ZGS) (Ref. 2) showed structures in $\Delta\sigma_L$, $\Delta\sigma_T$, and C_{LL} scattering in p-p mainly but also in some indirect p-n (through p-d) measurements. The new experiments from LAMPF,³ SIN,⁴ Saclay,⁵ Leningrad,⁶ and TRIUMF (Ref. 7) confirm the observed structures for energies lower than $T_p=0.8$ GeV. These were interpreted as being the signature of 1D_2 and 3F_3 dibaryonic resonances from the various phase shift analysis.⁸ The inelastic channels⁹ are particularly interesting since it was shown that calculations¹⁰ based on unitary relativistic three body models¹¹ are unable to reproduce some experimental data, especially for spin transfer parameters K_{NN} and K_{LL} (Ref.

12) and others.¹³

Several theoretical predictions¹¹ have been made which generally conclude that the structures in the data and loops in the Argand plots were produced by non-resonant dynamics coupling to $N-\Delta$ and $NN\pi$. Although generally believed, this negative conclusion on the existence of the dibaryon resonances was not supported by all calculations.¹⁴ A work from Jauch *et al.*¹⁵ in particular showed that an admixture of dibaryon resonance $L=1, J^P=3^-$, in addition to calculations from the Deck model leads to a good description of such data as $\Delta\sigma_L^{\text{inel}}$ and inelastic total NN cross sections otherwise badly described. However an alternative explanation in terms of heavy meson exchange has been proposed.¹⁶

The pion-deuteron physics concerns mainly the $pp \rightarrow d\pi^+$ studies and elastic π -d scattering with measurements of differential cross sections, vector polarization iT_{11} and tensor polarization T_{20} . The $\bar{p}p \rightarrow d\pi^+$ experiments, which study analyzing powers and differential cross sections have been developed¹⁷ at Saturne (Saclay), LAMPF, SIN, TRIUMF, and Gatchina. A detailed discussion can be found in Seth.¹⁸ These results have been analyzed¹⁹ using either phase shifts or coupled channel equations allowing a simultaneous analysis of NN, π d, $N\Delta$, and $NN\pi$ channels. Although the fit between mea-

sured and calculated data is poor, it is possible to reach a conclusion on the existence of dibaryons from these discrepancies.^{20,21} The vector analyzing power iT_{11} in the $\pi d \rightarrow pp$ reaction has been measured at SIN.²² The qualitative agreement found with theoretical predictions does not require us to invoke the existence of dibaryons. Similarly the lack of agreement between the measurements¹³ of the spin correlation parameter A_{NN} in $pp \rightarrow d\pi^+$ and theoretical predictions prevents us from drawing any conclusion about dibaryons.

The iT_{11} parameter in elastic π -d scattering has been carried out at SIN, using polarized deuterium targets. While the first data²³ showed the oscillatory behavior often attributed to dibaryons, more recent data²⁴ are smooth. The analysis has been done within relativistic three body theory²⁵ and Faddeev amplitudes.²⁵

The tensor polarization T_{20} in elastic π -d scattering has been measured at SIN,²⁶ LAMPF,²⁷ and TRIUMF.²⁸ The experimental results are contradictory, although very close incident energies and angles were investigated. The data show oscillations at some energies at SIN but a smooth and negative behavior at LAMPF and TRIUMF.

The polarization of the proton produced in deuteron photodisintegration measurements in Tokyo²⁹ was, together with NN studies, the earliest contribution to the dibaryon hunt. At least two resonances, one isoscalar and one isovector have been found. The first Japanese results appear however to be in contradiction³⁰ either with theoretical calculations or new photodisintegration measurements. After analysis of new differential cross sections measurements of $\gamma d \rightarrow pn$, $\gamma d \rightarrow \pi^0 d$, and $\gamma d \rightarrow pX$ reactions, the authors were not able to draw a clear conclusion about the existence of dibaryon resonances.

The above discussion deals with broad dibaryons with widths of the order of $\Gamma_{1/2} \approx 100-200$ MeV. But interest has however moved gradually toward narrow resonances. McGregor,³¹ analyzing the masses and quantum numbers of the resonances of the structures from NN experiments, concluded they were rotational levels based on a virtual $pp\pi$ dibaryon bound state at 2.02 GeV. He predicted a 3P_1 level at 2.06 GeV. Wainer and Lomon,³² analyzing the constraints imposed by all the experimental informations in the energy region through the phase shifts, found that the required width of such a postulated resonance should be $\Gamma < 0.3$ MeV. Later Mulders,³³ using the P matrix formalism to connect the short range part of the interaction described by six quarks in a bag with the long range part of the interaction (the long range part of the Paris potential) predicted some very narrow dibaryonic states.

Experimental studies were undertaken which led to negative results. Total n-p cross sections have been measured at LAMPF,³⁴ studying invariant masses lying between $1.93 < \sqrt{S} < 2.23$ GeV. Although the statistics and energy resolution were good, no evidence in narrow resonances was reported. Other negative studies have been reported which will be discussed more carefully later. They are the p-p elastic scattering cross section at $\theta_{c.m.} = 90^\circ$,³⁵ using an internal gas jet target at Saturne

(Saclay), $2.12 < \sqrt{S} < 2.40$ GeV, the $d(\pi^+, p)p$ relative yield³⁶ measured at LAMPF at $\theta_{c.m.} = 90^\circ \pm 2^\circ$, in the range $2.07 < \sqrt{S} < 2.28$ GeV and the measurement of analyzing power in $d(p, p')pn$ reaction from LAMPF (Ref. 36) at $\theta_{lab} = 18^\circ$, in the range $2.00 < \sqrt{S} < 2.07$ GeV.

Measurements with positive signals come from different kinds of experiments. They will be discussed in Sec. IV G. Various review articles have been published on this subject of dibaryonic resonances.¹⁸

II. EXPERIMENTAL METHOD

The experiment was performed at the Laboratoire National Saturne (LNS) using the proton beam delivered by the Saturne synchrotron. Some preliminary data were taken in 1979. More extensive measurements were done one year later in 1980. In both studies, differential cross sections for ${}^3\text{He}(p, d)X$ were measured. Then, in June 1983, complementary measurements were done by exchanging the incident and target particles: $p({}^3\text{He}, d)X$ at roughly the same center of mass energy. In all three cases, the outgoing deuteron was detected in the spectrometer SPES1 and identified by a 5.6 m basis time of flight added to the p/z measurement. The missing mass M_x was given by the angle and the momentum of the deuteron. One magnetic field setting covered $\approx 3\%$ of $\Delta p/p$ (≈ 30 MeV in M_x). Many different settings with large overlaps were used in order to get a large missing mass spectrum of several hundred MeV. The different parts of the experiment description will be detailed in the following paragraphs. Data acquisition has been made with the S.A.R. computer³⁷ specially developed for fast acquisition.

A. Beam transport and spectrometer

Figure 1 shows the beam line corresponding to the energy loss SPES1 spectrometer.³⁸ Three quadrupoles located before the target allow the adjustment of the beam line for the kinematic of the studied reaction. In our case, due to the relatively small dimensions of the cryogenic target, we have focused the beam onto the target. It follows that the currents in all quadrupoles remain constant for a given energy. The sextupoles were not used, and the collimators were not moved during the measurements at a given angle. The current in the spectrometer SPES1 was adjusted to get the measurements for different momenta of the detected particles which correspond to different missing masses for the undetected $B=2$ system (X). The magnetic fields in the spectrometer and analyzer were regulated within some parts in 10^5 , and checked using NMR signals.

The quadrupole located between the target and the spectrometer, was adjusted in order to keep the vertical angular aperture $\Delta\theta_v$ constant. The position of the beam was determined using wire chambers and secondary emission detectors. The centering on the target was also checked by measuring the counting rate as a function of the horizontal position of the beam. The stability in position during the measurements was controlled with a localization wire chamber located before

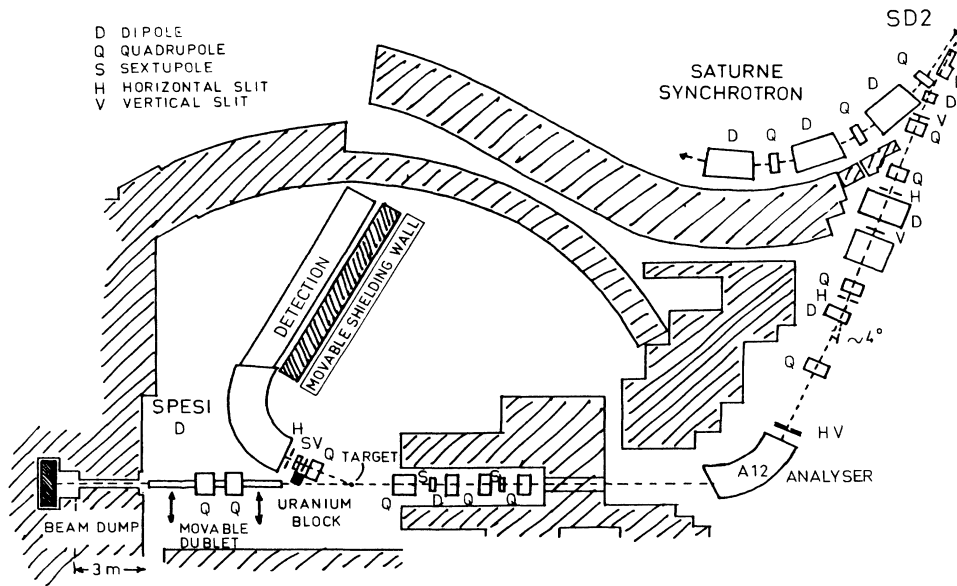


FIG. 1. Beam line.

the target, and checked between every data taking. The stability was better than ± 1 mm.

B. Target

The liquid ${}^3\text{He}$ target was constructed by the IPN cryogenic service.³⁹ The target cell was a cylinder 50 mm in diameter and 68.8 mm in length kept at a pressure of 300 Torr. The corresponding temperature was 2.425 ± 0.025 K, and the thickness $\rho d = 509 \pm 9$ mg/cm². Three windows were crossed successively by the protons and deuterons at small angles: stainless steel (20 μm), aluminum (10 μm), and Kapton (75 μm). The L H_2 target was constructed by the LNS cryogenic group. Its thickness was 205 ± 20 mg/cm².

C. Monitoring

Two different telescopes and a secondary electron emission chamber were mainly used for the beam calibration. The telescope M1, located in the vertical plane at 30° to the beam direction, was made of six scintillation counters. The telescope M3 was made of four scintillation counters heavily shielded by lead, and located in the horizontal plane at 90° from the beam. A secondary emission monitor was located before the target in the direct beam, and not viewed by the spectrometer for the angles considered here.

The ratios of the counting rates between these three monitors was checked to be stable within $\pm 1\%$. In the few cases where this limit was exceeded they have been corrected and 20% of that correction introduced in the error bar. The absolute calibration was done at each energy by means of the activation reaction $\text{C}(p, X){}^{11}\text{C}$ or $\text{C}({}^3\text{He}, X){}^{11}\text{C}$.⁴⁰ A typical value of the beam intensity was 15 nA at large angle decreasing to 0.25 nA at small

angle. The beam duration for 0.925 GeV protons was close to 600 ms every 1320 ms.

D. Detectors

Four double drift chambers⁴¹ were used to determine the trajectory of each detected deuteron (see Fig. 2). Each chamber consists of one drift cell 50 cm long corresponding to $\Delta P/P = \pm 2\%$. In fact due to the loss of precision at both ends of the detection, only a part of the detection covering roughly 3% of the mean momentum was used. The trigger consisted of five planes of scintillation counter hodoscopes. The time-of-flight information for particle identification was measured between planes *F* and *A* on a 5.6 m basis. Figure 3 shows two typical time-of-flight spectra, corresponding to the situations with few protons on detection, and with a large amount of protons. Note the enhancement of the scale in order to point out the base line of the spectra.

E. Choice of measurements

Since the best kinematical conditions to look for possible narrow structures are not known, measurements have been done at different angles and energies. Conditions corresponding to large momentum transfers seem to be favorable because they correspond to a frontal scattering. However the production cross section may be larger at smaller angles. It is obviously the ratio of the production cross section versus the cross section of the background which is the important factor.

Data for the reaction ${}^3\text{He}(p, d)X$ have been measured at two energies $T_p = 0.925$ and $T_p = 0.750$ GeV and different angles, from $M_x \approx 1.88$ to $M_x \approx 2.35$ GeV. At $T_p = 0.925$ GeV, the experimental deuteron angles were

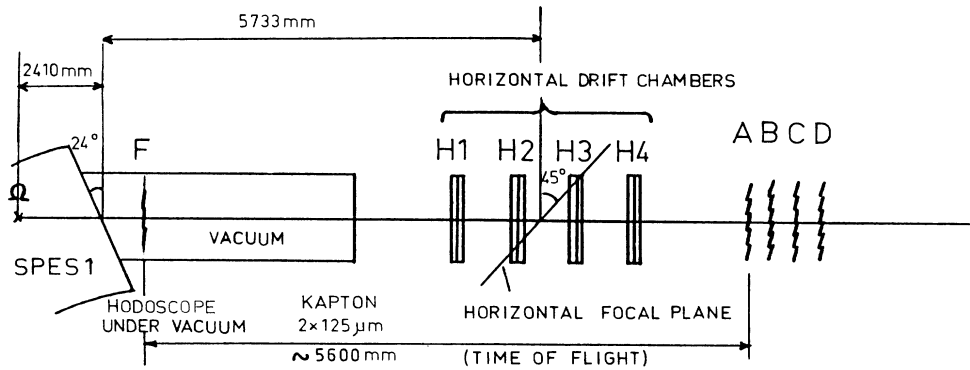


FIG. 2. Layout of the detection system (not to scale). *A*, *B*, *C*, *D*, and *F* are scintillation counter hodoscopes. Ω is the (virtual) source point for trajectories entering the spectrometer along its optical axis.

40° and 30° , and at $T_p = 0.750$ GeV, $\theta_d = 40^\circ$, 32° , and 22° .

Measurements were also done at 6° for $T_p = 0.75$ GeV showing in particular a peak at $M_x \approx 1.9$ GeV corresponding to a quasifree scattering of the incident proton on a deuteron substructure of ${}^3\text{He}$. The data show also a peak for $M_x = 2.09$ GeV corresponding to the quasifree $pp \rightarrow d\pi^+$ reaction. For this range of missing masses the magnetic field in the spectrometer is larger than that corresponding to elastically scattered protons, which occurs at $M_x = 2.15$ GeV. The proton flux was then so large for this small angle, that measurements were stopped for $M_x = 2.13$ GeV. At this small angle furthermore, the spectrometer coils were protected from direct beam by an uranium block which produced a large background in the detection. Consequently the data for $T_p = 0.750$ GeV and $\theta_d = 6^\circ$ will not be presented later.

Measurements were also done at $\theta_d = 14^\circ$ for $T_p = 0.925$ and 0.750 GeV. At this angle the data were more sparse at 0.925 GeV. Moreover this angle corresponds to the maximum laboratory angle possible for the quasifree $pp \rightarrow d\pi^+$ reaction. The deuterons so produced contaminated the spectrum in a large range of

missing masses, starting at $M_x \approx 2.2$ GeV. This contamination appeared unfortunately to be not negligible, especially at $T_p = 0.750$ GeV, in comparison with the small yield of the expected structures, so the data for this angle and the two energies will not be discussed later.

For the $p({}^3\text{He},d)X$ reaction data have been measured at $T_{3\text{He}} = 2.7$ GeV and $\theta_d = 18^\circ$ lab. This energy corresponds to total c.m. energy close to the previous one. The lower branch of the kinematical curve has been chosen so that the $\theta_{\text{c.m.}}$ for (p,d) system have neighboring values for both reactions.

F. Data reduction

1. Proton contamination

At all angles, the proton flux increases very quickly for the magnetic fields corresponding to elastic scattering on ${}^3\text{He}$. The protons were cut electronically by the time of flight, but since their flux was larger than deuteron flux by a factor up to 50, we have checked that no peak in the deuteron spectrum occurs due to a very small leak of the protons in the deuteron time-of-flight peak. Since a proton peak could only occur for elastic scattering, we have shown the corresponding missing mass in the figures by an arrow noted p. We can see that no peak appears for these particular conditions. In Fig. 3 two typical time-of-flight spectra are shown, demonstrating that the proton contamination under the deuteron peak is equal or less than 2% depending on the magnetic field value in the spectrometer.

The quasifree $pp \rightarrow pp$ reaction on a proton in ${}^3\text{He}$ cannot be at the origin of the narrow structures we will present later for ${}^3\text{He}(p,d)X$ spectra. There are different reasons for that: the very good separation between p and d in time of flight, the kinematics which never corresponds, the width of $pp \rightarrow pp$ which will be very broad.

A two step process like $p{}^3\text{He} \rightarrow {}^3\text{He}p$, followed by a stripping of ${}^3\text{He}$ giving final d, can be also excluded. Indeed the kinematics do not correspond for a reaction at angle θ followed by stripping at 0° . Moreover the widths here also should be very large because all angles

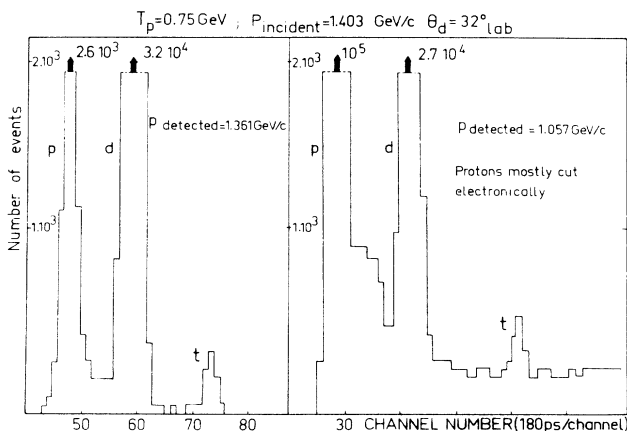


FIG. 3. Typical time-of-flight spectra.

(in three dimensions) are allowed for the first process, followed by the complementary angle for the second one. Table I shows the deuteron momenta in laboratory system for all these processes, compared with the deuteron momenta of the structure that will be described later. One can see that the only contamination could come from $pd \rightarrow dp$ process on a deuteron substructure of ${}^3\text{He}$. We suspect the widths of the peaks due to this last process to be somewhat broader than the peaks we observe. Although the protons are cut by the time-of-flight measurement, the momenta of protons from quasielastic pp scattering are also indicated in Table I.

2. Angular acceptance

Slits at the entrance of the spectrometer defined the following angular apertures: $\Delta\theta_v = 51.8$ mrad and $\Delta\theta_H = 48.9$ mrad. However due to the size of the detection, some trajectories were not detected. Each trajectory was defined by the eight chambers, determining its angle: θ_f , and its intersection y with a virtual plane. Then the analyzing code using θ_f and y calculated the corresponding missing mass M_x and the angle of the emitted deuteron from the target θ_d . All events for each run were plotted in a bidimensional spectrum $N = f(\theta_d, M_x)$. For a heavy target, without recoil, the focal plane is located in the middle of the drift chambers (Fig. 2) and the shape of the bidimensional spectrum defining the horizontal acceptance, looks similar to a parallelogram. For the reaction we have studied, the recoil is very important, especially at large angles. As the angle varied, the focal plane moved to infinity and came back from the forward direction. The trajectories undergo strong cuts at large angles for small missing masses and at small angles for large missing masses—as shown in Fig. 4. The computer code consequently calculated the horizontal opening angle—permitted by the detection—for each bin (corresponding to 1 MeV precision in energy scale of M_x) of each run. Both extremi-

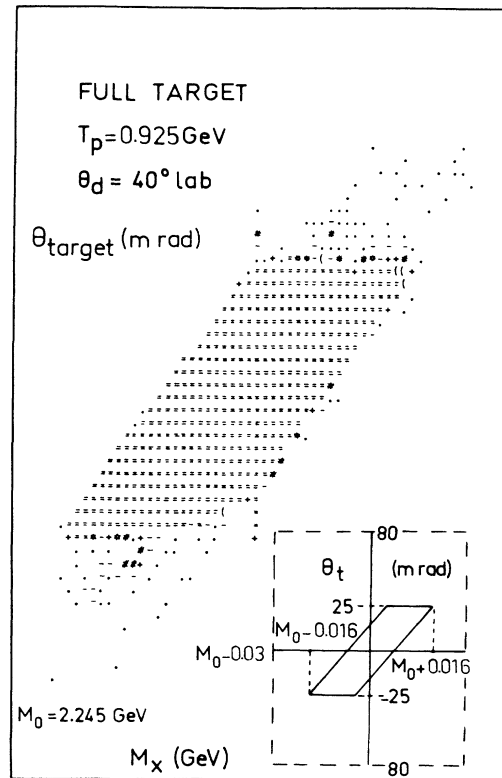


FIG. 4. Deuterons of a single measurement at 40° , $T_p = 0.925$ GeV, displayed on a bidimensional plot θ vs M_x , and strongly saturated (the symbol = represents seven events) in order to show the background around the useful region. The scales of the spectrum are indicated in the inset.

ties of this parallelogram, which have small statistics and poorly determined $\Delta\theta_H$, were omitted by software cuts. For each bin an error bar for the horizontal opening angle was computed (see below, Sec. II F 6) simultaneously with the angle itself.

TABLE I. Kinematical conditions for all processes suspected to give the observed structures. Note that $pp \rightarrow d\pi$ is impossible, the maximum deuteron angle being much smaller than the angles considered here.

Reaction	T_{beam} (GeV)	θ_d^{lab} (deg)	p_{beam} (GeV/c)	p_d peak (GeV/c)	p_d (GeV/c) $pd \rightarrow dp$	p_d (GeV/c) ${}^3\text{He} \rightarrow {}^3\text{He}p$ ${}^3\text{He} \rightarrow dp(0^\circ)$ a	p_p (GeV/c) $pp \rightarrow pp$
${}^3\text{He}(p,d)X$	0.925	40	1.6098	1.1555 ($M_x = 2.24$) 1.3423 ($M_x = 2.124$)	1.388	1.062	1.024
${}^3\text{He}(p,d)X$	0.925	30	1.6098	1.3920 ($M_x = 2.192$)?	1.625	1.227	1.241
${}^3\text{He}(p,d)X$	0.750	40	1.4035	0.9989 ($M_x = 2.192$)	1.245	0.9496	0.9228
${}^3\text{He}(p,d)X$	0.750	32	1.4035		1.410	1.0658	1.070
${}^3\text{He}(p,d)X$	0.750	22	1.4035	1.2855 ($M_x = 2.155$)?	1.580	1.183	1.232
$p({}^3\text{He},d)X$	2.7	18	4.7387	1.366 ($M_x = 2.24$)	2.588 ^b	2.188	1.438 ^c
			$p_{\text{beam}}/3 = 1.5796$		0.831	1.504	

^aCorresponds to ${}^3\text{He}(p,{}^3\text{He})p$ at θ_{lab} followed by ${}^3\text{He} \rightarrow p + d$ at 0° ($p_d = \frac{2}{3}p_{{}^3\text{He}}$).

^bCorresponds to $p(d,d)p$ with $p_d = \frac{2}{3}p_{{}^3\text{He}}$.

^cCorresponds to $T_p = \frac{1}{3}T_{{}^3\text{He}}$ quasifree elastic scattering.

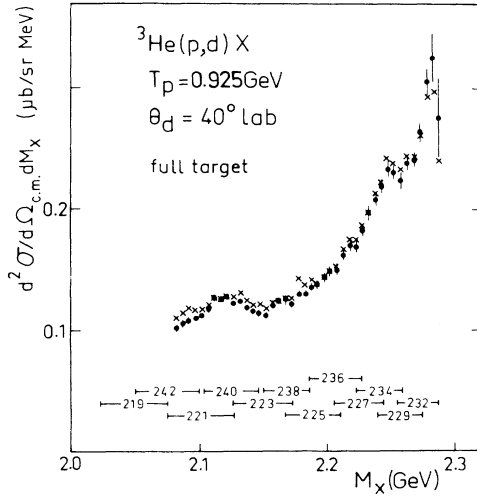


FIG. 5. Overlap of different runs to obtain the missing mass spectra for $2.085 < M_x < 2.28$ GeV, and the effect of a correction factor $(1/\sigma)(d\sigma/d\theta) = 3.6 \times 10^{-3}/\text{mrad}$: ● (without correction: ×).

3. Summation of runs

In order to avoid possible systematic errors each spectrum results from several different runs with large overlap, as seen in Fig. 5. The data from adjacent spectrometer settings agree within the statistical uncertainties in the region of overlap. A spectrum is then obtained by mixing the different data using the usual statistical relations. The same analysis was done for full and empty targets and subtracted. When not specified, the results correspond to full-minus-empty target measurements. At small angles the counts from the empty target were negligible in comparison with the full target, and consequently were measured less systematically. The subtraction was therefore not made. For the data shown later this is the case only for $T_p = 0.750$ GeV, $\theta_d = 22^\circ$.

4. Angular correction

Because of the shape of the acceptance (Fig. 4), all missing masses within a given run are measured with slightly different average scattering angles. However due to the large overlap of the runs, the final spectrum is insensitive to the angular correction (see Fig. 5). A small correction was nevertheless applied to all data.

5. Losses due to counting rate

Dead time can produce a loss of counting rate at different stages of the data acquisition. This loss was measured on line by the comparison of the number of events simulated on the detectors by a pulse generator and the number of events registered by the computer. The generator was triggered by a signal of a photomultiplier of a monitor telescope detector and therefore followed all beam intensity fluctuations. This correction was checked by repeating a measurement with a beam

whose intensity was increased by a factor of 7. The final results after counting loss corrections agree within a few percent. The proton intensity was varied for different production angles and usually adjusted to keep the dead time below 15%.

6. Error estimation

The statistical errors are computed using different factors coming from full and empty target countings. The uncertainty on the horizontal aperture was taken to be $(NC + 0.5)^{-1}$ where NC corresponds to the number of channels in the angular axis of the bidimensional spectrum used to define the aperture itself. Sometimes a correction had to be introduced because the time-of-flight spectrum showed a non-negligible background under the deuteron time of flight peak. This correction was $< 2\%$ and a term corresponding to 20% of this correction factor was introduced in the error bar. In the same way 20% of a possible factor correcting monitors fluctuation was also introduced. All these factors computed statistically gave the error bars plotted on the figures, typically less than or equal to $\pm 3\%$, allowing us to conclude that a high statistics experiment had been undertaken. There is in addition, not introduced in the data shown, a systematic error coming principally from the absolute calibration of the monitors, but also from the vertical opening angle and the target thickness known to $\pm 1.8\%$. It can be estimated to be $\pm 15\%$.

7. Missing mass resolution

From kinematics we obtain the following relations:

$$\Delta M_x = \frac{\partial M_x}{\partial p_3} \Delta p_3 + \frac{\partial M_x}{\partial \theta_3} \Delta \theta_3$$

with

$$\frac{\partial M_x}{\partial p_3} = \frac{p_1 \cos \theta_3 - E_0 \beta_3}{M_x}$$

and

$$\frac{\partial M_x}{\partial \theta_3} = -\frac{p_1 p_3 \sin \theta_3}{M_x},$$

where $E_0 = E_1 + m_2$ and the notations 1, 2, 3, and x refer to the projectile, target, detected deuteron, and missing mass, respectively. The contribution of $\partial M_x / \partial E_1$ is small and can be neglected.

The main contribution to ΔM_x comes from $(\partial M_x / \partial \theta_3) \Delta \theta_3$ because of the beam focusing conditions. This term increases with angle. For a given angle it decreases for increasing missing masses because M_x increases and simultaneously $p_3 \equiv p_d$ decreases. There is also a noticeable contribution due to target thickness which again increases with angle.

At two angles and energies ($T_p = 0.925$ GeV, $\theta_d = 40^\circ$ and $T_p = 0.750$ GeV, $\theta_d = 32^\circ$), the counting rate corresponding to protons elastically scattered on ^3He was small enough to allow its measurement (there were no cuts applied by the electronics). The corresponding

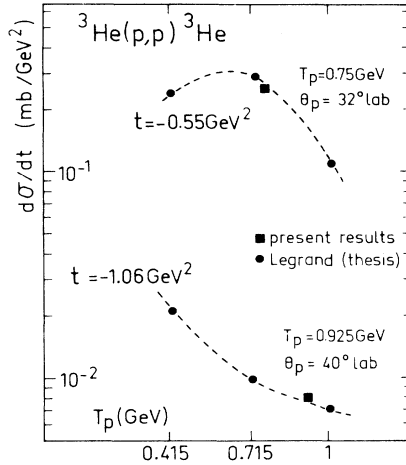


FIG. 6. ${}^3\text{He}(p,p){}^3\text{He}$ elastic scattering cross sections.

cross sections are plotted on Fig. 6 and compared with data from Legrand.⁴² The $d\sigma/dt$ values agree with the interpolated values within 6–8%. The energy resolution of these elastic proton peaks is used to check the computed values of the energy resolution which is strongly dependent on $\Delta\theta_3$. The resolutions agree roughly, which allows us to conclude that our energy resolution for the ${}^3\text{He}(p,d)X$ reaction varied from $\Delta M_x \approx 3$ MeV at $\theta_d = 22^\circ$, to $\Delta M_x \approx 7-8$ MeV at $\theta_d = 40^\circ$. These values are for missing masses, close to $M_x \approx 2.24$ GeV, but are not very different for slightly smaller missing masses where structures have also been found. The missing mass resolution for $p({}^3\text{He},d)X$ reaction at $\theta_d = 18^\circ$ is close to 4 MeV. These values justify our choice of analyzing the data with a value of 1 MeV for each energy bin. Then, after having checked that no structure narrower than 10 MeV was present, an integration of the spectra was done, in order to increase the statistical precision. The data presented have been binned into 5 MeV intervals.

8. Missing mass calibration

There is a direct and known correspondence between the magnetic field measured by means of NMR and the momentum of the detected deuterons. For a given spectrum an overall small correction constant has been applied to all data to correct for energy loss of protons and deuterons in the target. It usually ranges between -2 to -3 MeV. A very good agreement with the ${}^3\text{He}$ mass had been found in the ${}^3\text{He}(p,p){}^3\text{He}$ elastic scattering reported before. We conclude that our energies are correct to better than 2 MeV.

III. RESULTS

We present here the results from all our measurements. To extract cross sections for appearing structures we used the procedure usually employed in high energy physics⁴³ to obtain the values quoted in Table II. First a polynomial fit has been carried out after having removed the five data points corresponding to clearly appearing structures. Then the number of standard deviations (SD) from the background has been computed using the relation

$$SD = \sum_i [(N_{Ti} - N_{Bi}) / \Delta\sigma_i^2] / \left[\sum_i 1 / \Delta\sigma_i^2 \right]^{1/2}$$

where N_{Ti} corresponds to the total cross section for the data i , N_{Bi} the corresponding value for the background got by means of the polynomial fit described previously, and $\Delta\sigma_i^2 = \Delta\sigma_{Ti}^2 + \Delta\sigma_{Bi}^2 \approx 2\Delta\sigma_{Ti}^2$. $\Delta\sigma_{Ti}$ corresponds to the total error bar. Values of masses, widths, cross sections, and corresponding precisions are determined by using all the data and making Gaussian fits in addition to the previous polynomial fit.

A. $T_p = 0.925$ GeV, $\theta_d = 40^\circ$ (Fig. 8)

Two sets of data (N79 and N80) have been taken a year apart. A bump located close to $M_x = 2.243$ GeV is observed in the missing mass spectrum. The analysis of

TABLE II. Number of standard deviations (SD) from the background of the narrow structure. The masses (M_x), total widths at half maximum ($\Gamma_{1/2}$), and cross sections ($d\sigma/dt$) correspond to the structures found.

	Angle	SD	M_x (GeV)	$\Gamma_{1/2}$ (GeV)	$d\sigma/dt$ ($\mu\text{b}/\text{GeV}^2$)	$-t$ (GeV^2)
$M_x = 2.24$ GeV						
$p({}^3\text{He},d)X$	17.64°	3.10	2.245 ± 0.002	0.016 ± 0.003	7.3 ± 2.0	
$T_{3\text{He}} = 2.7$ GeV	18°	1.40	2.237 ± 0.002	0.015 ± 0.004	2.8 ± 1.1	-0.04
	18.36°	0.74	2.232 ± 0.003	0.018 ± 0.007	2.5 ± 1.4	
${}^3\text{He}(p,d)X$						
$T_p = 0.925$ GeV (N80)	40°	2.73	2.243 ± 0.003	0.017 ± 0.006	1.3 ± 0.57	0.96
$T_p = 0.925$ GeV (N79)	40°	5.64	2.241 ± 0.002	0.024 ± 0.004	2.32 ± 0.50	0.96
$M_x = 2.12$ GeV						
$T_p = 0.925$	40°	6.94	2.121 ± 0.001	0.025 ± 0.002	1.46 ± 0.15	0.89
$M_x = 2.19$ GeV						
$T_p = 0.750$ GeV	40°	4.13	2.192 ± 0.003	0.025 ± 0.006	4.16 ± 1.34	0.63

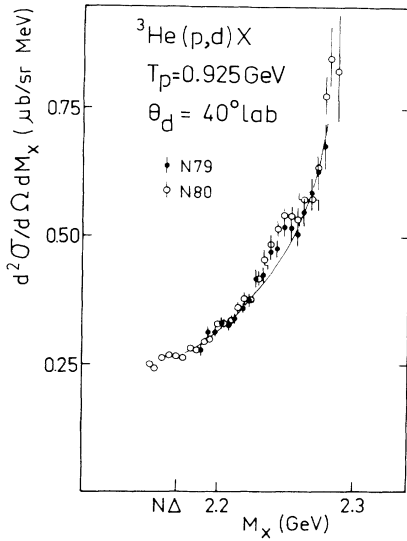


FIG. 7. Comparison of some results obtained at different dates.

both sets of data, shown in Fig. 7, indicates a very good agreement. Indeed both have been quantitatively corrected for the background giving close values for M_x , $\Gamma_{1/2}$, and $d\sigma/dt$ as indicated in Table II.

The spectrum in Fig. 8 shows a broad bump corresponding to the quasifree $pd \rightarrow dp$ scattering of incident protons as a deuteron substructure of ${}^3\text{He}$. It shows also an increase in background corresponding to the opening of the $N\Delta$ channel. The phase space has been calculated for $X=pp$ and $N\Delta$, but the first one gives a small contribution since it has to be normalized at low invariant masses $M_x=2.0$ GeV where the cross section is very small. The contribution of phase space $X=N\Delta$

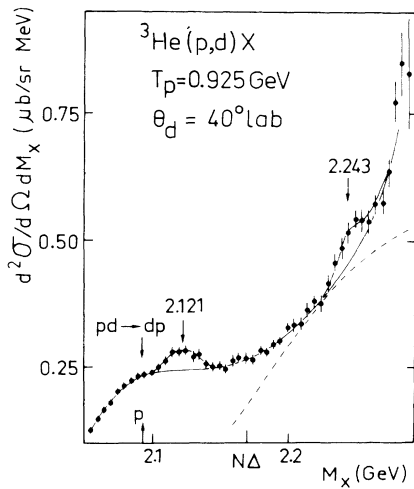


FIG. 8. Missing mass spectra for $T_p=0.925$ GeV and $\theta_d=40^\circ$ lab. The full curves correspond to polynomial and polynomial plus Gaussian fits. The dashed curve is the normalized phase space ($X=N\Delta$, $\Gamma_{1/2}=0.115$ GeV for the Δ). Data have been binned into 5 MeV intervals.

TABLE III. ΔM : shift (in MeV) between the experimental maximum of the peak observed in ${}^3\text{He}(p,d)X$, associated with the $pd \rightarrow dp$ reaction on d substructure, and the same for free reaction. W : width of the peak (in MeV).

	θ_d (lab deg)	ΔM	W
$T_p=0.75$ GeV	6	5	44
	14	4	56
	22	3	69
	32	9	67
	40	14	88
$T_p=0.925$ GeV	30	2	68
	40	0	79

($\Gamma_{1/2}=0.115$ GeV), normalized to our data, is shown by dashed curve. It appears clearly to be unable to fit the measured cross sections.

Two narrow structures are clearly seen at $M_x=2.121$ and 2.243 GeV. Note that the X^2 obtained by ignoring the 2.121 GeV narrow structure but with a shift of the $pd \rightarrow dp$ broad bump to 2.1 GeV ($\Delta M=9$ MeV instead of 0 MeV in Table III) is worse by a factor of 4 in the missing mass region $2.0 \leq M_x \leq 2.2$ GeV.

B. $T_p=0.750$ GeV, $\theta_d=40^\circ$ (Fig. 9)

For this lower energy, we see again a large bump corresponding to $pd \rightarrow dp$, and a structure at 2.192 GeV. The 2.12 GeV region being in a dip it is difficult to say something. The measurements have been stopped at an overly small missing mass, preventing a study of the structure seen previously at 2.240 GeV. The dashed curve corresponds again to the normalized phase space for $X=N\Delta$ ($\Gamma_{1/2} \approx 115$ MeV) (Fig. 9), where it can be seen that there is no structure in this phase space spectrum at the corresponding masses. The empty target spectrum is shown in Fig. 10. There is no structure in this spectrum at $M_x=2.192$ GeV. The ratio of full to empty target countings for the two aforementioned structures is larger than 4.5.

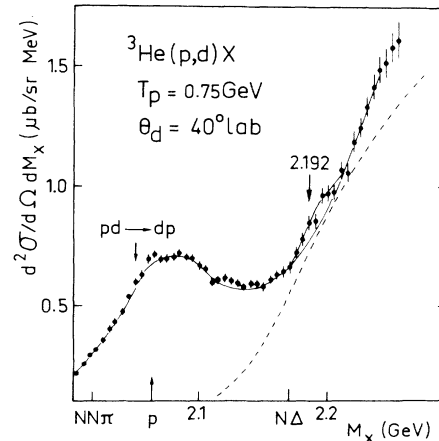


FIG. 9. Same as Fig. 8, but for $T_p=0.75$ GeV.

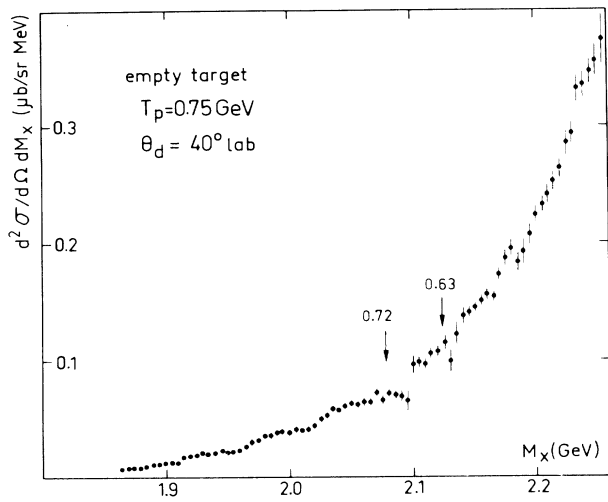


FIG. 10. Corresponding empty target spectrum. The arrows show the full-minus-empty target cross section.

C. $T_p=0.925$ GeV, $\theta_d=30^\circ$ (Fig. 11)

Apart from the $pd \rightarrow dp$ bump, some very weakly excited structures are seen, but the lack of statistics prevents any precise interpretation of the data (Fig. 11). Nothing can be firmly deduced from this spectrum, although the arrow drawn at 2.192 GeV show that the spectrum is compatible with structure for that mass.

The phase space curve shown corresponds to $N\Delta$ final state ($\Gamma_{1/2}=115$ MeV). A phase space prediction with four particles in the final state (d, p, p, and π) has also been calculated using the code FOWL.⁴⁴ Its predictions, normalized on the data, are similar to the one drawn on Fig. 11.

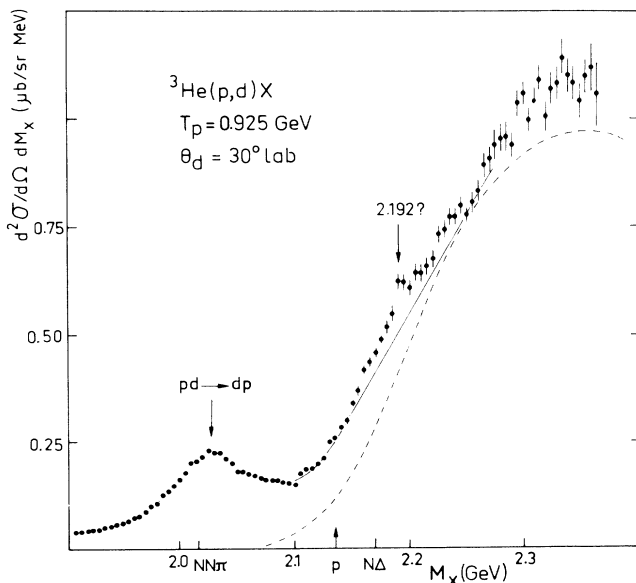


FIG. 11. Same as Fig. 9 for dashed curve, but for $T_p=0.925$ GeV, $\theta_d=30^\circ$ lab. The solid line is drawn by hand.

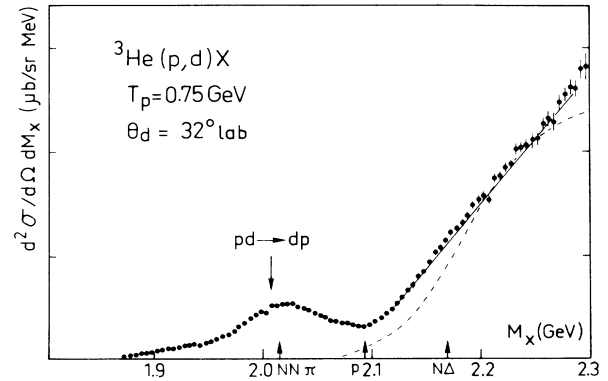


FIG. 12. Same as Fig. 11, but for $T_p=0.75$ GeV, $\theta_d=32^\circ$ lab.

D. $T_p=0.750$ GeV, $\theta_d=32^\circ$ (Fig. 12)

The bump corresponding to $pd \rightarrow dp$ is the only dominant feature of this spectrum (Fig. 12). Within the error bars, there is no room here for any narrow or broad structure. The phase space for $X=N+\Delta$, again does not fit the measured differential cross sections.

E. $T_p=0.750$ GeV, $\theta_d=22^\circ$ (Fig. 13)

The spectrum (Fig. 13) shows the $pd \rightarrow dp$ bump, and a broad structure centered around $M \approx 2.14$ GeV ($\Gamma_{1/2} \approx 115$ MeV) with $d\sigma/d\Omega \approx 142$ $\mu\text{b}/\text{sr}$. The full lines have at this stage been drawn by hand to guide the eye. The empty target cross sections, which are very small for small angles, require only a few measurements. Both sets of data are presented on Fig. 13. No fit has been done on the data but the spectrum is compatible with a structure at 2.155 GeV as indicated by an arrow.

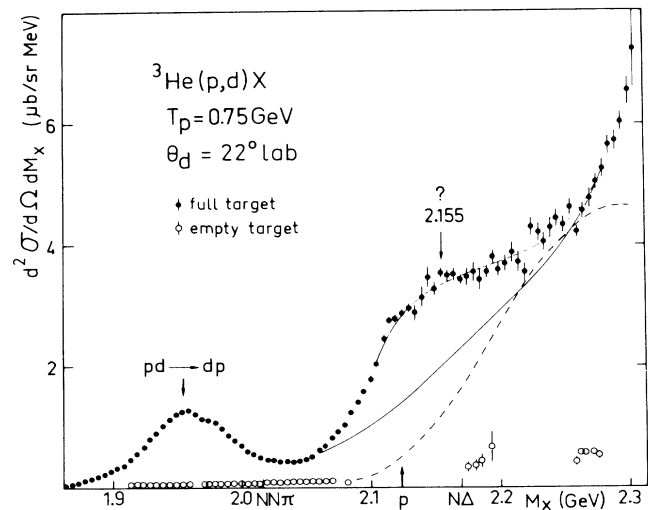


FIG. 13. Same as Fig. 11, but for $T_p=0.75$ GeV, $\theta_d=22^\circ$ lab.

F. $p(^3\text{He}, d)X$ reaction at $T_{^3\text{He}} = 2.7$ GeV (Fig. 15)

In order to check that the structures observed were not a consequence of possible parasitic scattering on some windows, or slits, a measurement of the reaction inverting the roles of beam and target seemed very useful. The energy was chosen in order to have a total center of mass energy as close to that of the previous reactions at $T_p = 0.925$ GeV as was allowed by the dipole of the transport beam line. The laboratory angle for the detected deuterons $\theta_d = 18^\circ$, corresponds to the only angular region free of $p(p, d)\pi^+$ reaction and, for the missing masses studied, far from the maximum of the laboratory angle (Fig. 14). The $p(p, d)\pi^+$ reaction quoted will be a quasifree reaction with a proton from incident ^3He particles having one third of the energy and momentum.

The results already published,⁴⁵ are recalled on Fig. 15. They show broad bumps centered around 2.17 GeV ($M_N + M_\Delta$), depending on the curve drawn to reproduce the background (Fig. 16), and a small structure centered around $M_x \approx 2.240$ GeV. Figure 16 shows phase space calculations for $X = NN$ and $N\Delta$ normalized to our data. The NN final state phase space increases with M_x , in contradistinction to the $^3\text{He}(p, d)X$ reaction, since in $p(^3\text{He}, d)X$ the center of mass is moving quickly in the laboratory due to the large ratio of incident particle mass to the target particle. The full lines correspond to the background used to extract the cross sections of the narrow and broad structures.

In Fig. 14, three curves are drawn to show the kinematical conditions corresponding to $p(p, d)\pi^+$; the one without Fermi motion of a p in ^3He , and two others, with a p having a Fermi motion of ± 100 MeV/c along the beam direction. If we allow the Fermi motion of the projectile nucleon to have any direction, there is indeed a small probability that deuterons coming from this elementary process will enter the spectrometer. However their momentum distribution is wide and cannot give rise to a narrow structure as the one observed here. The same argument holds for the previous cases when the ^3He is the target nucleus: a contamination from the quasifree $pN \rightarrow d\pi$ reaction is possible at the lowest angle ($\theta_d = 22^\circ$), but this cannot create narrow structures in the missing mass spectrum.

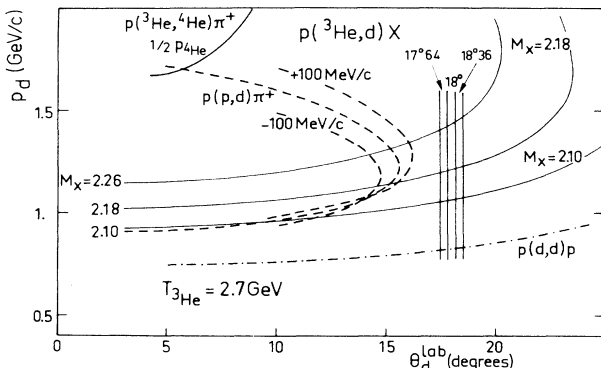


FIG. 14. Kinematics for $p(^3\text{He}, d)X$ reaction.

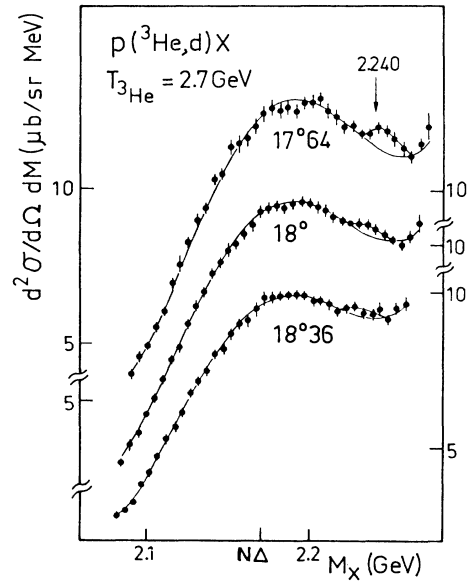


FIG. 15. Missing mass spectra for $p(^3\text{He}, d)X$ reaction at $T_p = 2.7$ GeV and $\theta_d = 17.64^\circ$, 18° , and 18.36° . The solid lines correspond to polynomial and polynomial + Gaussian fits.

Now let us ask the question if the observed peak was produced by a parasitic target heavier than liquid hydrogen. Of course the data from the empty target have been subtracted. Moreover if the target is somewhat heavier than hydrogen, the momentum of the deuterons created by means of $^3\text{He}(p, d)$ reaction at $\theta_{\text{lab}} = 18^\circ$ and $T_{^3\text{He}} = 2.7$ GeV, increases immediately with the target mass to a value outside the experimental range. For example for $d(^3\text{He}, d)^3\text{He}$ (g.s.) $p_d = 3.65$ GeV/c, and in order to have $p_d = 1.35$ GeV/c, we have to consider an excited state in ^3He as high as 1.0 GeV. We have there-

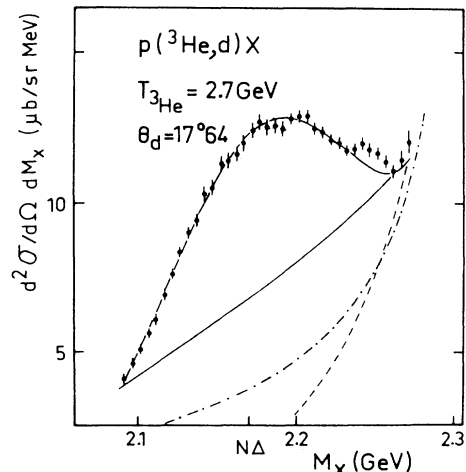


FIG. 16. Normalized phase space calculations for $p(^3\text{He}, d)X$ reaction. The dashed curve (dot-dashed) corresponds to $X = N\Delta$ ($\Gamma_{1/2} = 0.115$ GeV) ($X = NN$). The solid curves correspond to polynomial fit and a curve drawn by hand to obtain the broad bump excitation cross section.

fore no explanation for the small shift of the missing mass with angle in the $p(^3\text{He},d)X$ reaction. In particular we do not think that it can be explained by local inefficiencies of the detection since many runs with slight differences in magnetic field of the spectrometer are combined as explained in Sec. II F 3 and Ref. 45. In any case, the spectrum obtained by averaging the three angle spectra presented in Fig. 15 still exhibit a bump close to 2.236 GeV with four standard deviations. The slight improvement compared to each of the three individual standard deviations is due to the summation of statistics.

IV. DISCUSSION

A. Quasifree $pd \rightarrow dp$ process

The position of the maximum of the quasifree $pd \rightarrow dp$ peak is strongly dependent on the background subtraction which presents an important slope. Results of Table III show the value of the shift between the experimental maximum of the peak observed in $^3\text{He}(p,d)X$, associated with reaction on d substructure in ^3He , $pd \rightarrow dp$, and the position of the maximum predicted by kinematics for a free reaction. This determination is not very precise because of the background subtraction. The mean value of the shift is larger than 5 MeV, not far from the ^3He binding energy (7.7 MeV). In Table III, we indicate the total width at half maximum again not very precise because of background. One can observe an increase with angle, for a given energy.

B. State at $M_x = 2.24$ GeV

It has been quantitatively determined from $p(^3\text{He},d)X$ data at 17.64° and 18° , and practically not seen at 18.36° . Both sets of data for $^3\text{He}(p,d)X$ reaction at $T_p = 0.925$ GeV and $\theta_d = 40^\circ$ show a structure for this invariant mass. The masses deduced are stable if the data at 18.36° is omitted. The final mass value is $M_x = 2.240 \pm 0.005$ GeV, with $\Gamma_{1/2}$ [full width at half maximum (FWHM)] $\approx 18 \pm 3$ MeV.

No structure was seen for this invariant mass in the deuteron breakup experiment,⁴⁶ but this mass corresponds to the limit of that experiment, where the counting rate for each bin is very small (< 10). Some other measurements done with high energy resolution, such as $d(p,p)pn$,³⁶ $d(\pi,p)p$,³⁶ or $d(\pi,\pi)d$ (Ref. 26) have not been extended to an invariant mass as large as 2.24 GeV.

Jauch *et al.*¹⁵ analyzing different NN data, have shown that an introduction of a dibaryon admixture $T=1, J^P=3^-$ to the Deck model helps in obtaining good agreement with experimental data for $\Delta\sigma_L(pp \rightarrow NN\pi)$ and various total cross sections $\sigma(NN \rightarrow NN\pi)$. They predicted a dibaryon mass of 2.236 GeV, precisely the one measured here, but with $\Gamma_{\text{tot}} = 120$ MeV and $\Gamma_{\text{el}} = 26$ MeV. Let us recall however, that addition of ρ meson exchange in the isobar models can explain the data.¹⁶

C. State at $M_x = 2.121$ GeV

Its mass, width, and production cross section $d\sigma/dt$ for the $^3\text{He}(p,d)X$ reaction have been determined at $\theta_d = 40^\circ$ for 0.925 GeV. Results are shown in Fig. 17 and Table II. In deuteron breakup experiments,⁴⁶ the structures observed at 2.137 ± 0.01 GeV (M_{np}), 2.11 ± 0.02 GeV (M_{nn}) have masses consistent with 2.121 GeV. So is the structure observed at 2.137 ± 0.015 GeV (M_{pp}) in the ^4He breakup experiment (dppn final states), and at 2.126 ± 0.015 GeV (M_{pp}) (pppp π^-n final state⁴⁷).

No peak for such invariant mass was observed in the $d(\pi,p)p$ (Ref. 36) experiment. However we notice that the large t value $t \approx 0.4$ GeV² does not seem favorable for the excitation of this peak. It is close to the t value for $p(^3\text{He},d)X$ reaction at $T_{^3\text{He}} = 2.7$ GeV, $\theta_d = 18^\circ$ ($t = 0.32$ GeV²), where that structure was also absent.

D. State at $M_x = 2.192$ GeV

It has been analyzed quantitatively at $T_p = 0.750$ GeV, $\theta_d = 40^\circ$ (see Table II), and it could exist in the spectrum shown at $T_p = 0.925$ GeV, $\theta_d = 30^\circ$. The t values for both cases are rather large (respectively, -0.627 GeV² and -0.422 GeV²). A peak at this mass value has never been seen previously.

E. Bump at $M_x \approx 2.17$ GeV

A large bump with a mass close to 2.17 GeV and a width of the order of $\Gamma_{1/2} \approx 110$ MeV was observed at $T_p = 0.75$ GeV, $\theta_d = 22^\circ$ in the $^3\text{He}(p,d)X$ reaction and $T_{^3\text{He}} = 2.7$ GeV, $\theta_d = 18^\circ$ in the $p(^3\text{He},d)X$ reaction. In both cases the invariant cross sections $d\sigma/dt$ are of the order of several hundred $\mu\text{b}/\text{GeV}^2$, typically two orders of magnitude larger than the narrow structures discussed before. These two reactions for the given angles and en-

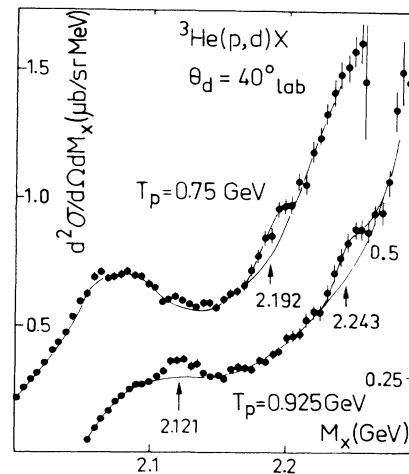


FIG. 17. Missing mass spectra for $^3\text{He}(p,d)X$ reaction at $T_p = 0.925$ and 0.750 GeV, $\theta_d = 40^\circ$ lab showing the presence of the states at $M_x = 2.121$, 2.192 , and 2.243 GeV.

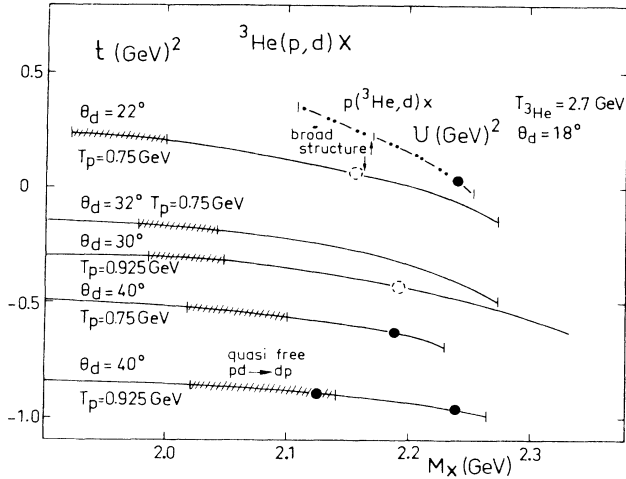


FIG. 18. Domain of missing mass (M_x) and transfer (t) covered in our measurements. The solid circles give the position of observed structures, while the open circles refer to indications for a structure.

ergies, have the smallest momentum transfers of the different experimental conditions of the data reported here (Fig. 18).

Since the broad bump was not observed for other angles and energies, we conclude that its excitation cross section is a quickly decreasing function of momentum transfer. Since its mass is close to the mass of free $M_N + M_\Delta$, and width close to the width of free Δ , we identify that broad bump with $N + \Delta$ in final state interaction.

F. Inelasticity of the narrow structures

Some NN experiments have been done with high statistical accuracy and energy resolution. Among them are the following.

(i) p-p differential cross section at 90° c.m. with internal gas jet target from Saturne,³⁵ where invariant masses from 2.12 to 2.40 GeV have been studied with high momentum transfer ($-0.9 < -t < -0.5$ GeV²).

(ii) p-p analyzing powers using the radiography experimental setup at LNS,⁴⁸ where invariant masses from 2.18 to 2.33 GeV have been explored to ($0.65 < T_p < 1.0$ GeV; $16^\circ < \theta^{\text{lab}} < 36^\circ$).

(iii) $\sigma_T(n-p)$ from LAMPF,³⁴ though with less precise experimental conditions for invariant masses close to 2.2 GeV.

Since now narrow structure appeared in these high energy resolution experiments, we deduce that the corresponding elasticities are small.

G. Results observed in other experiments

Some structures have been suggested at other masses. The deuteron breakup experiment⁴⁶ analysis, concluded

the existence of structures for the following masses: $M_x \approx 2.02 \pm 0.01$ GeV ($\Gamma_{1/2} = 0.045 \pm 0.02$ GeV) for M_{np} invariant mass, $M_x \approx 2.03 \pm 0.02$ GeV ($\Gamma_{1/2} \approx 0.075 \pm 0.02$ GeV) for M_{NN} invariant mass, and $M_x \approx 2.39 \pm 0.02$ GeV ($\Gamma_{1/2} \approx 0.06 \pm 0.02$ GeV) for $M_{NN\pi^+}$ invariant mass. We should notice that the analysis of deuteron breakup experiment from Tokyo,⁴⁹ more recent but with again very poor statistics, is not in agreement with the data presented by the Warsaw group.⁴⁶ The ^4He breakup experiment analysis⁴⁷ with (dppn) final state, reported the existence of a structure in the invariant mass of two protons at 2.035 ± 0.015 GeV ($\Gamma_{1/2} \approx 0.030 \pm 0.023$ GeV), identified with 3.0 standard deviations. The ^4He breakup experiment analysis⁴⁷ with (pppp π^- n) final state reported a peak for a pp invariant mass of 2.036 ± 0.015 GeV ($\Gamma_{1/2} \approx 0.027 \pm 0.025$ GeV). A pion production experiment (pp \rightarrow d π^+) (Ref. 50) from LNS reported a narrow structure for $T_p = 0.35$ GeV which corresponds to an invariant mass of 2.044 GeV. There is also a narrow structure at 2.014 GeV reported⁵¹ from Bonn in two protons invariant mass studied by means of $\gamma d \rightarrow pp\pi^-$ experiment. The two proton invariant mass observed using incident 5 GeV/c pions on ^{12}C (propane bubble chamber) at Dubna, revealed a peak for a mass (FWHM) of 2.024 ± 0.003 GeV (0.021 ± 0.015 GeV).⁵² The same experiment using 40.0 GeV/c π^- observed a peak for a mass (FWHM) of 2.026 ± 0.0066 GeV (0.032 ± 0.005 GeV).⁵³ The d breakup experiment using 3.3 GeV/c d, revealed peaks at following masses (FWHM): 2.014 ± 0.01 GeV (0.063 ± 0.028 GeV) and 2.162 ± 0.01 GeV (0.018 ± 0.026 GeV).⁵⁴ There is an indication of a peak at 2.171 GeV (Ref. 55) in $n + p \rightarrow pp\pi^+\pi^-\pi^-\pi^0$ experiment, done with 5.1 GeV/c neutron beam in Dubna. Finally, in the two protons invariant mass studied with C(p,2p)X reaction, peaks have been observed at 2.115, 2.155, and 2.235 GeV with a total width $\Gamma_{1/2}$ of the order of 15 to 35 MeV.⁵⁶ Notice that, as quoted at the beginning of the paper, some other experiments have not observed any structure. A complete review of experiments on this subject for masses larger than 2.00 GeV has been made elsewhere.⁵⁷

H. General discussion

All data, those collected during the experiments $^3\text{He}(p,d)X$ and $p(^3\text{He},d)X$ and those recalled in the previous section have been plotted in Fig. 19. Are these states created by strong $N\Delta$ coupling? One such state has been predicted theoretically⁵⁸ in the analysis of π -nucleus scattering, but no theory can explain the existence of many of them. One argument favors such a hypothesis: a search for isoscalar dibaryons⁵⁹ has not been able to find them with a limit, on $d\sigma/dt$, of a few tenths of nb/GeV². This is two orders of magnitude lower than the excitation cross sections found in the $B=2$, $T=1$ search described in this paper. The experiment was a missing mass measurement from $d + d \rightarrow d + X$ reaction. However, since incident and target deuterons are loosely bound structures, their large radii can lead to a strong reduction of the production cross sections.⁶⁰ Then, in spite of the fact that we have

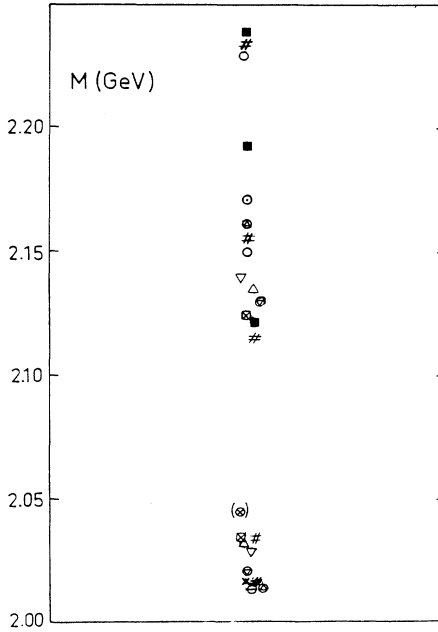


FIG. 19. Display of the narrow dibaryon masses found in the different experiments. The data are from: ■, this work; ○, Agakishiev *et al.* (Ref. 53); #, Andronenko *et al.* (Ref. 56); ⊙, Glagolev *et al.* (Ref. 54); ⊙, Besliu *et al.* (Ref. 55); △, Glagolev *et al.* (Ref. 47); ×, Bairamov *et al.* (Ref. 52); ⊕, Siemiarczuk *et al.* (Ref. 46); ⊠, Zelinski *et al.* (Ref. 47); ▽, Siemiarczuk *et al.* (Ref. 46); ⊖, Bock *et al.* (Ref. 51); and ⊗, Saudinos *et al.* (Ref. 50).

not been able to observe isoscalar dibaryon resonances in an experiment especially designed to see them, we will not consider the $N\Delta$ explanation for the dibaryons observed here. The main reason is that we think it is difficult to understand how the large width $\Gamma_{1/2} \approx 0.115$ GeV of the Δ resonance can be so reduced when bound with only one nucleon. The coupling of Δ with nuclei generally leads to a smaller reduction of the width remaining as large as 55–60 MeV.⁶¹

The dibaryon at 2.121 GeV has a mass lower than $M_N + M_\Delta$ (~ 2.17 GeV). It will most probably deexcite into $NN\pi$. Since the $N-\pi$ interaction in s state is rather “weak,” the relatively small width of this state can be qualitatively understood. An explanation relating the dibaryons observed to interferences between different partial waves amplitudes has been proposed. For example, Hollas,⁶² using the Mandelstam prediction⁶³ that singlet NN partial waves produce pions at a lower momenta than do triplet partial waves, concluded that no resonant behavior was required to describe the structures observed in $\Delta\sigma_T$ and $\Delta\sigma_L$. However such an explanation disagrees with the observed features in our experiment of several narrow peaks stable in mass for different kinematical conditions and not symmetric with regard to $M_N + M_\Delta = 2.17$ GeV. A narrow quasibound state was predicted some years ago by Arenhövel,⁶⁴ as formed by the $(N\Delta)$ system. Since it was at a mass lower than 2.17 GeV (2.13–2.16 GeV) and with isospin $T=2$ (forbidding decay into the NN channel) such an explanation is not

satisfactory in our case. It is obvious that more theoretical effort has to be done within such a model to be more conclusive.

Another way to explain the existence of the observed narrow dibaryons is to describe them as states of six quarks coupled in a configuration other than q^3-q^3 . Many theoretical works have been done in this framework, usually within the MIT-type bag model.¹ Many states are then predicted. Few authors have tackled the problem of the calculation of their widths: Dorkin *et al.*,⁶⁵ using a coupled channel method between six quarks and NN channels, have found for a simplified assumption of a single state of six quarks in S wave, a width close to 20 MeV for NN scattering at $T_p=0.3$ GeV. Matveev⁶⁶ predicted the contribution of a single gluon exchange process to a hidden color state to the width to be close to 10 MeV. We notice that the calculated values of widths are close to the experimental ones presented in this work. Grein *et al.*⁶⁷ have calculated the dibaryons relative decay into π^+d and π^+np . We believe that a theoretical understanding of the widths of the states discussed here may have fundamental implications connected to the confinement of quarks.

Recent theoretical investigations, including pionic corrections to a six quark bag calculation,⁶⁸ predict masses different from those found experimentally. A prediction based on 6 quarks shell model in a jj coupling combined with a diquark cluster model⁶⁹ found 2.13 and 2.24 GeV for the position of the two first levels in very good agreement with some levels found in our work. Since in this theoretical work there is a partial degeneracy in spin and total degeneracy in isospin, too few levels have been found. The NN partial width predicted in the last theoretical work quoted is small, but there is no prediction for total widths.

V. CONCLUSION

We have measured missing mass spectra from ${}^3\text{He}(p,d)X$ and $p({}^3\text{He},d)X$ reactions leading to $T_x=1$ and $B_x=2$ final states. The quasifree scattering on the deuteron substructure of ${}^3\text{He}$ is clearly observed at all angles and energies. The good statistics and missing mass resolution for this inelastic channel with large momentum transfer, allows the observation of narrow states. These narrow states were observed although they stand on top of a relatively large background formed by nonresonant $N\Delta$ and $NN\pi$ final states. Individual peaks are not present for all kinematical conditions (angle and energy). The relative excitation of the peaks and background, in addition to the experimental precision, allow the observation of these narrow structures only for some t values (see Fig. 18). The nonobservation of these structures in some experiments [and some angles in ${}^3\text{He}(p,d)X$ measurements] is then related to kinematically unfavorable conditions. The states observed are either in a quark configuration different from q^3-q^3 , or in a q^3-q^3 extraneous state (quantum numbers forbidding NN decay without quark rearrangement). This can be considered as being an experimental signature of quark effects at intermediate energies.

ACKNOWLEDGMENTS

We wish to thank T. Bauer, F. Samaran, and N. Willis for help in the writing of the computer code analysis.

We wish to thank F. Sai, J. Saudinos, and W. J. Schwillie for communicating their data to us prior to publication. We thank C. Wilkin for stimulating discussions and help in writing this paper.

- ¹R. J. Jaffe and F. E. Low, *Phys. Rev. D* **19**, 2105 (1979); A. Th. M. Aerts *et al.*, *ibid.* **17**, 260 (1978); P. J. G. Mulders *et al.*, *ibid.* **21**, 2653 (1980); P. J. G. Mulders *et al.*, *Phys. Rev. Lett.* **24**, 1543 (1978); C. W. Wong and K. F. Liu, *ibid.* **41**, 82 (1978); K. F. Liu and C. W. Wong, *Phys. Lett.* **113B**, 1 (1982); C. W. Wong *et al.*, *Phys. Rev. C* **22**, 2523 (1980); S. M. Dorkin *et al.*, Dubna Report P4-81-791, 1981 (in Russian).
- ²A. Yokosawa, *Phys. Rep.* **64**, 47 (1980); I. P. Auer *et al.*, *Phys. Lett.* **70B**, 475 (1977); I. P. Auer *et al.*, *Phys. Rev. Lett.* **41**, 354 (1978); Y. Makdisi *et al.*, *ibid.* **45**, 1529 (1980); I. P. Auer *et al.*, *Phys. Rev. D* **24**, 2008 (1981); I. P. Auer *et al.*, *Phys. Rev. Lett.* **46**, 1177 (1981); I. P. Auer *et al.*, *ibid.* **48**, 1150 (1982); G. R. Bureson *et al.*, *Nucl. Phys. B213*, 365 (1983); W. R. Ditzler *et al.*, *Phys. Rev. D* **27**, 680 (1983); I. P. Auer *et al.*, *ibid.* **29**, 2435 (1984).
- ³I. P. Auer *et al.*, *Phys. Rev. D* **29**, 2435 (1984); T. S. Bhatia *et al.*, *Phys. Rev. Lett.* **49**, 1135 (1982).
- ⁴E. Aprile-Giboni *et al.*, *Phys. Rev. D* **27**, 2600 (1983); *Phys. Rev. Lett.* **46**, 1047 (1981).
- ⁵J. Bystricky *et al.*, *Phys. Lett.* **142**, 130 (1984).
- ⁶V. A. Andrew *et al.*, *Yad. Fiz.* **35**, 1457 (1982) [*Sov. J. Nucl. Phys.* **35**, 852 (1982)]; A. V. Dobrovolsky *et al.*, *Nucl. Phys. B214*, 1 (1983).
- ⁷D. Axen *et al.*, *J. Phys. G* **7**, L225 (1981); A. S. Clough *et al.*, *Phys. Rev. C* **21**, 988 (1980); J. P. Stanley *et al.*, *Nucl. Phys. A403*, 525 (1983).
- ⁸J. Bystricky *et al.*, *Nuovo Cimento* **82**, 385 (1984); K. Hashimoto *et al.*, *Prog. Theor. Phys.* **64**, 1678 (1980); H. Hidaka *et al.*, *Phys. Lett.* **70B**, 479 (1977); K. Hashimoto and N. Hoshizaki, *Prog. Theor. Phys.* **64**, 1693 (1980); D. V. Bugg *et al.*, *Phys. Rev. C* **21**, 1004 (1980).
- ⁹I. P. Auer *et al.*, *Phys. Rev. Lett.* **51**, 1411 (1983); A. D. Hancock *et al.*, *Phys. Rev. C* **27**, 2742 (1983); T. Rupp *et al.*, *ibid.* **28**, 1696 (1983); T. S. Bhatia *et al.*, *ibid.* **28**, 2071 (1983).
- ¹⁰J. Dubach *et al.*, *Phys. Rev. C* **34**, 944 (1986).
- ¹¹W. M. Kloet and R. R. Silbar, *Nucl. Phys. A364*, 346 (1981); J. H. Gruben and B. J. Verwest, *Phys. Rev. C* **28**, 836 (1983); B. J. Verwest and R. A. Arndt, *ibid.* **25**, 1979 (1982); W. Grein and P. Kroll, *Nucl. Phys. A377*, 505 (1982); W. Grein *et al.*, *Phys. Lett.* **96B**, 176 (1980); W. M. Kloet *et al.*, *ibid.* **99B**, 80 (1981); W. M. Kloet and J. A. Tjon, *ibid.* **106B**, 24 (1981); F. Shimizu *et al.*, *Nucl. Phys. A389*, 445 (1982); T. Ueda, *Phys. Lett.* **141B**, 157 (1984); W. M. Kloet and R. R. Silbar, *Phys. Rev. Lett.* **45**, 970 (1980); V. S. Bhasin and I. M. Duck, *Nucl. Phys. B64*, 289 (1973); B. Blankleider and I. R. Afnan, *Phys. Rev. C* **24**, 1572 (1981); B. J. Edwards and G. H. Thomas, *Phys. Rev. D* **22**, 2772 (1980); T. Ueda, *Phys. Lett.* **74B**, 123 (1978); **119B**, 281 (1982); M. Araki *et al.*, *Nucl. Phys. A389*, 605 (1982); J. A. Niskanen, *Phys. Lett.* **112B**, 17 (1982); W. M. Kloet and J. A. Tjon, *Nucl. Phys. A392*, 271 (1983); J. A. Tjon and E. Van Faassen, *Phys. Lett.* **120B**, 39 (1983); W. M. Kloet and J. A. Tjon, *Phys. Rev. C* **27**, 430 (1983); S. Y. Tsai, *Prog. Theor. Phys.* **64**, 1710 (1980); L. A. Kondratyuk and I. S. Shapiro, *Yad. Fiz.* **12**, 401 (1970) [*Sov. J. Nucl. Phys.* **12**, 220 (1971)]; R. Bhandari *et al.*, *Phys. Rev. Lett.* **46**, 1111 (1981); M. Rosina and H. J. Pirner, *Nucl. Phys. A367*, 398 (1981); H. Sato and K. Saito, *Phys. Rev. Lett.* **50**, 648 (1983); M. Cvetic-Krivec *et al.*, *Phys. Lett.* **99B**, 486 (1981).
- ¹²G. Glass *et al.*, *Phys. Lett.* **129**, 27 (1983).
- ¹³G. Glass *et al.*, *Phys. Rev. Lett.* **53**, 1984 (1984).
- ¹⁴B. J. Edwards, *Phys. Rev. D* **23**, 1978 (1981).
- ¹⁵W. Jauch, A. Konig, and P. Kroll, *Phys. Lett.* **143B**, 509 (1984); L. G. Dakhno *et al.*, *ibid.* **114B**, 409 (1982).
- ¹⁶T. Ueda, *Prog. Theor. Phys.* **76**, 729 (1986).
- ¹⁷B. G. Ritchie *et al.*, *Phys. Rev. C* **24**, 552 (1981); B. Mayer, *et al.*, *Nucl. Phys. A437*, 630 (1985).
- ¹⁸R. R. Silbar, *Comments Nucl. Part. Phys.* **12**, 177 (1984); A. Svarc, *Nucl. Phys. A434*, 329c (1985); E. L. Lomon, Invited Talk at the Sixth International Symposium on High Energy Spin Physics, Marseilles, 1984, edited by J. Saffer [*J. Phys. (Paris)* (in press)]; P. Kroll (unpublished); K. K. Seth, in *Proceedings of the International Conference on High Energy Photonuclear Reactions and Related Topics*, Tokyo, 1983, edited by S. Homma and F. Sakata (INS, Tokyo, 1983); and unpublished.
- ¹⁹H. Garcilazo, *Phys. Rev. Lett.* **45**, 780 (1980); J. A. Niskanen, *Phys. Lett.* **141B**, 301 (1984); D. V. Bugg, *J. Phys. G* **10**, 717 (1984); **10**, 47 (1984); J. Dubach *et al.*, *Phys. Lett.* **106B**, 29 (1981); M. M. Makarov *et al.*, *ibid.* **122B**, 343 (1983); A. V. Kravtsov *et al.*, *J. Phys. G* **9**, L187 (1984); T. Mizutani *et al.*, *Phys. Lett.* **107B**, 177 (1981).
- ²⁰M. G. Dosh *et al.*, *Phys. Rev. C* **29**, 1549 (1984); H. Garcilazo, *Phys. Rev. Lett.* **48**, 577 (1982); E. Ferreira and G. A. Perez Munguia, *J. Phys. G* **9**, 169 (1983); A. S. Rinat and J. Arvieux, *Phys. Lett.* **104B**, 182 (1981); A. Matsuyama and K. Yazaki, *Nucl. Phys. A* **364**, 477 (1981); W. Grein and M. P. Locher, *J. Phys. G* **7**, 1355 (1981); K. Kubodera *et al.*, *ibid.* **6**, 171 (1980); J. Arvieux and A. S. Rinat, *Nucl. Phys. A350*, 205 (1980); K. Kubodera and M. P. Locher, *Phys. Lett.* **87B**, 169 (1979).
- ²¹M. Akemoto *et al.*, *Phys. Rev. Lett.* **51**, 1838 (1983); **50**, 400 (1983); J. H. Hoftiezer *et al.*, *Phys. Rev. C* **23**, 407 (1981); *Phys. Lett.* **100B**, 462 (1981).
- ²²G. G. Smith *et al.*, *Phys. Rev. C* **30**, 980 (1984).
- ²³J. Bolger *et al.*, *Phys. Rev. Lett.* **48**, 1667 (1982); **46**, 167 (1981).
- ²⁴E. L. Mathie *et al.*, *Phys. Rev. C* **28**, 2558 (1983); G. R. Smith *et al.*, *ibid.* **29**, 2206 (1984).
- ²⁵H. Garcilazo, *Phys. Rev. Lett.* **53**, 652 (1984); A. S. Rinat, *Phys. Lett.* **126B**, 151 (1983).
- ²⁶J. Ulbricht *et al.*, *Phys. Rev. Lett.* **48**, 311 (1982); W. Gruebler *et al.*, *ibid.* **49**, 444 (1982); V. Konig *et al.*, *J. Phys. G* **9**, L211 (1983).
- ²⁷E. Ungricht *et al.*, *Phys. Rev. Lett.* **52**, 333 (1984); E. Ungricht *et al.*, *Phys. Rev. C* **31**, 934 (1985).
- ²⁸G. R. Smith *et al.*, *Phys. Rev. Lett.* **57**, 803 (1986).
- ²⁹T. Kamae *et al.*, *Phys. Rev. Lett.* **38**, 468 (1977); T. Kamae and T. Fujita, *ibid.* **38**, 471 (1977); H. Ikeda *et al.*, *ibid.* **42**, 1321 (1979); *Nucl. Phys. B172*, 509 (1980).
- ³⁰K. Baba *et al.*, *Phys. Rev. Lett.* **48**, 729 (1982); *Phys. Rev. C*

- 28, 286 (1983); T. Ishii *et al.*, *Phys. Lett.* **110B**, 441 (1982).
- ³¹M. H. MacGregor, *Phys. Rev. Lett.* **42**, 1724 (1979); T. H. Fields and A. Yokosawa, *Phys. Rev. D* **21**, 1432 (1980).
- ³²J. Wainer and E. Lomon *Phys. Rev. D* **22**, 1217 (1980).
- ³³P. J. G. Mulders, *Phys. Rev. D* **25**, 1269 (1982); **26**, 3039 (1982); **28**, 443 (1983); P. J. G. Mulders, A. Th. M. Aerts, and J. J. De Swart, *Phys. Rev. Lett.* **40**, 1543 (1978).
- ³⁴P. W. Lisowski *et al.*, *Phys. Rev. Lett.* **49**, 255 (1982); R. E. Shamu *et al.*, *Phys. Rev. D* **25**, 2008 (1982).
- ³⁵M. Garcon *et al.*, *Nucl. Phys.* **A445**, 669 (1985).
- ³⁶K. K. Seth *et al.*, contributions from the Karlsruhe Conference on Few Body Problems in Physics, 1983, edited by B. Zeitnitz, p. 93.
- ³⁷B. Bricaud *et al.*, *IEEE Trans. Nucl. Sci.* **NS-26**, 4641 (1979).
- ³⁸J. Thirion *et al.*, Commissariat à l'Energie Atomique, Report N-1248, 1970; A. Boudard, Laboratoire National Saturne, Saclay, Internal report, 1980, p. D1.
- ³⁹S. Buhler, Proceedings of 8th International Cryogenic Engineering Conference, Berlin, 1980.
- ⁴⁰H. Quechon, Thèse de doctorat, Université Orsay, 1980.
- ⁴¹J. Saudinos *et al.*, *Nucl. Instrum. Methods* **111**, 77 (1973).
- ⁴²D. Legrand Thèse d'Etat, Université Paris-VI, 1979; R. Frascaria *et al.*, *Nucl. Phys.* **A264**, 445 (1976).
- ⁴³A. G. Frodesen *et al.*, *Probability and Statistics in Particle Physics* (Universitetsforlaget, Oslo, 1979), p. 406.
- ⁴⁴F. James, FOWL, European Organization for Nuclear Research Computer Centre, Program W-505.
- ⁴⁵B. Tatischeff *et al.*, *Phys. Rev. Lett.* **52**, 2022 (1984); B. Tatischeff *et al.*, Proceedings of the Xth International Conference on Particles and Nuclei, Heidelberg, 1984, edited by F. Güttner, B. Pouh, and G. zu. Putlitz, contributed paper C7.
- ⁴⁶T. Siemiarczuk *et al.*, *Phys. Lett.* **128B**, 367 (1983); T. Siemiarczuk *et al.*, *ibid.* **137B**, 434 (1984); B. S. Aladashvili *et al.*, *Nucl. Phys.* **A274**, 486 (1976).
- ⁴⁷V. V. Glagolev *et al.*, *Z. Phys.* **317**, 335 (1984); P. Zelinski *et al.*, Joint Institute for Nuclear Research Reports 1-83-565 and 1-83-566, 1983 (in Russian).
- ⁴⁸M. Garcon *et al.* *Phys. Lett.* **183B**, 273 (1987).
- ⁴⁹N. Katayama *et al.*, *Nucl. Phys.* **A423**, 410 (1984).
- ⁵⁰J. Saudinos *et al.*, Proceedings of the Nuclear Physics in the GeV Region Meeting, Tokyo, 1984.
- ⁵¹W. J. Schuille private communication, B. Bock *et al.*, *Nucl. Phys. A* **459**, 573 (1986).
- ⁵²A. A. Bairamov *et al.*, *Yad. Fiz.* **39**, 44 (1984) [*Sov. J. Nucl. Phys.* **39**, 26 (1984)].
- ⁵³H. N. Agakishiev *et al.*, *J. Nucl. Phys.* **41**, 1562 (1985) (in Russian).
- ⁵⁴V. V. Glagolev *et al.*, Joint Institute for Nuclear Research Rapid Communications, N5-84 (1984), p. 13.
- ⁵⁵C. Besliu *et al.*, Joint Institute for Nuclear Research, Report D1-815, 1983.
- ⁵⁶M. N. Andronenko *et al.*, Gatchina, 1986 Annual Report SG 96; A. A. Vorobyov, private communication.
- ⁵⁷B. Tatischeff *et al.*, *Europhys. Lett.* **4**, 671 (1987).
- ⁵⁸M. G. Huber, H. G. Hopf, and M. Dillig, in *Proceedings of the Workshop on Nuclear Physics with Stored, Cooled Beams—1984 (Spencer, Indiana)*, AIP Conf. Proc. No. 128, edited by P. Schwandt and H. O. Meyer (AIP, New York, 1984), p. 188.
- ⁵⁹M. P. Combes-Comets *et al.*, *Nucl. Phys.* **A431**, 703 (1984).
- ⁶⁰C. Wilkin, private communication.
- ⁶¹C. L. Morris *et al.*, *Phys. Lett.* **123B**, 37 (1983); C. Ellegaard *et al.*, *Phys. Rev. Lett.* **50**, 1745 (1983); B. Tatischeff *et al.*, *Phys. Lett.* **77B**, 254 (1978).
- ⁶²C. L. Hollas, *Phys. Rev. Lett.* **44**, 1186 (1980).
- ⁶³S. Mandelstam, *Proc. Phys. Soc. London, Sect. A* **244**, 491 (1958).
- ⁶⁴H. Arenhovel, *Nucl. Phys.* **A247**, 473 (1975).
- ⁶⁵S. M. Dorkin *et al.*, Dubna Report E2-80-43, 1980.
- ⁶⁶V. A. Matveev, Dubna Report D1,2-12036, 1978 (in Russian), p. 137.
- ⁶⁷W. Grein, K. Kubodera, and M. P. Locher, *Nucl. Phys.* **A356**, 269 (1981).
- ⁶⁸P. J. G. Mulders and A. W. Thomas, *J. Phys. G* **9**, 1159 (1983).
- ⁶⁹N. Konno *et al.*, *Lett. Nuovo Cimento* **34**, 313 (1982); N. Konno, private communication.